21PFL-0686

Quantitative Analysis of Gasoline Direct Injection Engine Emissions for the First 5 Firing Cycles of Cold Start

Jinghu Hu, Matthew Hall, and Ron Matthews University of Texas - Austin

Peter Moilanen, Steven Wooldridge, and Jianwen Yi Ford Motor Company

Abstract

A series of cold start experiments, using gasoline and iso-pentane fuels, were carried out for a 2.0 liter gasoline turbocharged direct injection (GTDI) engine to obtain the cold start emissions profiles for the first 5 firing cycles at an ambient temperature of 22°C. The exhaust gases, both emitted during the cold start firing and emitted during the cranking process right after the firing, were captured, and unburned hydrocarbon emissions (HC), CO, and CO_2 on a cycle-by-cycle basis during an engine cold start were analyzed and quantified. The HCs emitted during gasoline-fueled cold starts was found to reduce significantly as the engine cycle increased, while CO and CO_2 emissions were found to stay consistent for each cycle. Crankcase ventilation into the intake manifold through the positive-crankcase ventilation (PCV) valve system was found to have little effect on the emissions results. Cold start experiments fueled by highly volatile iso-pentane saw an overwhelming majority of the injected carbon captured in the exhaust gases, while a significant portion of the injected carbon during the gasoline-fueled cold starts was not captured. The comparative results not only validated the experimental methods, but also demonstrated that a significant fraction of the injected gasoline failed to evaporate during cold starts. During the first 5 firing cycles, 28% to 45% of the injected fuel mass was estimated to remain in the liquid phase and escaped capture. Because fuel could be carried over from one cycle to the next, in some cases, the actual unevaporated gasoline portion in a given cold start cycle could be even higher than that measured.

Introduction

Light-duty vehicle cold start emissions are currently a topic of great interest due to the need to meet stringent 2025 EPA regulations. Gasoline direct injection (GDI) features advantages over port-fuel injection (PFI) engines in various aspects including fuel economy, emissions reduction and cycle-by-cycle control possibility[1][2][3] and has been gaining increasing popularity. For model year 2019, GDI engines are found in 54% of the total light-duty U.S. vehicle fleet, compared with less than 3% in model year 2008 [4].

However, GDI engines produce high cold-start emissions, especially of unburnt hydrocarbons (HC)[5]. Cold-start emissions account for most of the total engine-out HC emissions during the U.S. Federal FTP test. During a cold start, the engine is started from a cold, static status and goes through a transient process in which the fuel rail pressure[6], the engine wall temperature[7] and engine speed increase before reaching the desired operating point. During this transient cold start process, suboptimal operation conditions, including low fuel rail pressure, low engine speed, and low cylinder temperature, result in liquid fuel wall deposition onto in-cylinder surfaces and a deterioration of the combustion during the first firing cycles[8]. The over-fueling injection strategy[9], which aims to compensate for the reduced gas-phase fuel concentrations causes more residual fuel in-cylinder and leads to higher HC emissions. The cold start process is characterized by large transients in engine parameters, and a more detailed, cycle-by-cycle or event-by-event optimization of the combustion parameters is needed to minimize the HC emissions.

There have been experimental ([3][10][11][12][13][14]) and simulation ([15][16][17]) research studies aiming to understand and possibly reduce the emissions during GDI engine cold starts. The first 5 firing cycle combustion events have been regarded as the most important in terms of cold start optimization. Based on the assumption that the cycle-by-cycle emissions data should remain consistent and similar during the test, a novel technique was developed in a previous research study [18] to isolate the emissions in each of the first 5 firing cycles and quantify the composition of emissions in each cycle. In research covered by this paper, a series of cold start experiments, with gasoline and iso-pentane as the fuel, were carried out and the results were analyzed to quantitatively determine emissions composition and the fate of the fuel in each of the firing cycles.

Experimental Methodology

Engine Specifications

Table 1 Engine Specification

Displacement	1999 cc
Bore/Stroke	87.5 mm/83.1 mm
Connecting Rod Length (Center to Center)	155.9 mm
Compression Ratio	10:1
IVO/IVC	10.9° ATDC/71.1 ABDC
EVO/EVC	55.1° BBDC/5.1 ATDC

Firing order	1-3-4-2

The engine of research interest was a model year 2017 Ford Escape 4-cylinder, 2.0-liter gasoline turbocharged direct injection (GTDI) engine. The variable valve timing (VVT) was disabled, and by default the intake valve was set to full retard and the exhaust valve to full advanced. A more detailed list of engine specification is shown in Table 1.

Experimental Setup

The engine and its peripherals were placed in an environmental chamber with the temperature controlled to 22±1 °C throughout the entire experiment. The experimental setup is shown in Figure 1. The experimental system could be divided into 3 parts: engine control and data acquisition, fueling, and exhaust gas collection and measurement. A water brake dynamometer was connected to the engine flywheel and provided a load similar to the in-vehicle engine load during idling.

Engine Control and Data Acquisition

The engine control unit (ECU) was replaced by a custom-developed National Instruments Labview Real-Time program which was deployed on the cRIO-9048 chassis and 7 cRIO modules placed in the chassis. The cRIO modules obtained and logged various engine parametric data from the ECU and controlled various powertrain relevant activities. A Siglent SDS1104X-E 4-channel oscilloscope was connected to the 4 in-cylinder piezoelectric pressure transducers which detected the instantaneous cylinder pressure. Oscilloscope signals were used to quantify the number of cycles the engine went through during a cold-start event.

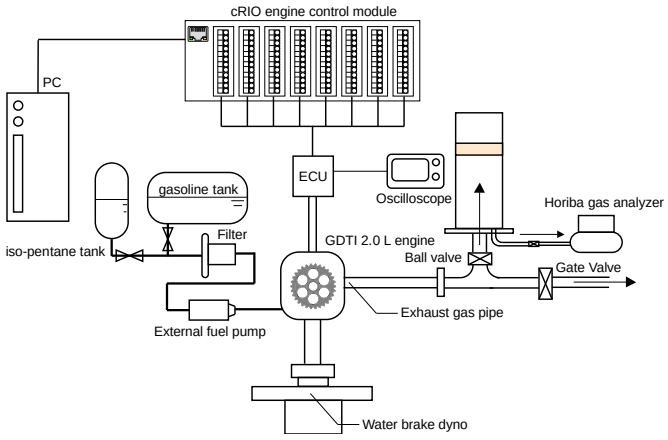

Figure 1 Schematic diagram of the engine cold start experiment

Fueling

Two fuel tanks, one storing gasoline and the other iso-pentane, were connected to the low-pressure fuel pump through valves on the fuel lines. As gasoline evaporation was far from ideal within the low temperature, low engine speed in-cylinder environment, part of the fuel would inevitably remain liquid and failed to be captured in the exhaust gases. With its boiling point of 27.8 °C at atmospheric pressure, iso-pentane evaporates rapidly after being injected into the cylinder and was expected to be fully combusted. Using iso-pentane provided validation of the current gas collection methodology and further insights of the fuel status in-cylinder. The external fuel pump was connected to the fuel line after a fuel filter and provided 2.7 bar of pressure and pumped the fuel, either gasoline or iso-pentane, to the high-pressure fuel pump of the engine.

Exhaust Gas Collection and Measurement

A two-way exhaust pipe system connected to the engine exhaust manifold was used to either capture the exhaust gas via the opening of a ball valve and closing of a gate valve, or direct it to the building exhaust system by switching the valve positions. The gas collection volume consisted of a 1 m tall, 19 cm inner-diameter acrylic cylinder, with a plastic foam piston sealing the cylinder. A Horiba MEXA-554JU gas analyzer was connected to the bottom of the cylinder through a 3/8'' NPT pipe fitting. During the cold start, the gate valve would be shut and the ball valve would be opened to allow the exhaust gas to flow into the acrylic cylinder and raise the piston. The trapped exhaust gas volume would be measured, and the gas would then be directed through the gas analyzer where its HC, CO and CO_2 molar concentrations were measured. The measured HC was in C_6(hexane) based.

Experiment Process

A validation experiment was carried out before the studies to check whether the exhaust gas collection equipment was able to collect all of the exhaust gas emitted through the exhaust manifold. The engine was cranked for a known number of cycles, the exact number quantified via the oscilloscope, and its emitted exhaust gas captured in the acrylic cylinder. The volume of the captured gas was measured and the per-cycle collected exhaust gas volume was calculated and validated against the theoretical per-cycle collected gas volume, which was obtained via the cylinder displacement volume and intake valve closing (IVC) timing.

For each experiment, the engine was first cranked for more than 10 cycles, the cranking exhaust gas collected and its HC, CO and CO_2 concentrations measured. This step, called pre-cold start cranking, was to quantify the in-cylinder residual fuel emission level. The pre-cold start cranking step was followed by a cold-start, during which the throttle was kept 15 degrees open. During a cold-start, 2 dummy cycles (cranking motored cycles without fuel or spark) were first applied for engine position synchronization. These 2 dummy cycles were then followed by a pre-defined number of firing cycles, during which fuel injection, spark ignition, and fuel pump activation were all enabled. After the targeted number of firing cycles was reached, all powertrain actions were disabled and the engine slowed down through several inertia cycles. Dummy cycles, firing cycles, and inertia cycles combined together to form a cold start. All the exhaust gas from the cold start was collected and analyzed. After the cold start was over, the engine was then cranked for more than 10 cycles, with the exhaust gas also captured and analyzed. This step was called post-cold start cranking. The objective of the post-cold start cranking step was to check for any residual combustion products, perhaps due to back-flow into the intake manifold and then back into the cylinder.

However, the gas captured during post-cold start cranking inevitably included some residual fuel deposited in the cylinder and crankcase. Hence, the per-cycle HC emissions during the pre- and post-cold start

cranking were compared in each experiment to understand the fate of the injected fuel mass.

The formal cold start experiments were carried out after the equipment validation experiments and the pre-cold start cranking experiment. Cold start experiments with the firing cycle number ranging from 1 to 5 were carried out. For each firing cycle number scenario, 5 parallel experiments were done, including one or two experiments with the positive crankcase ventilation (PCV) valve detached from the intake manifold to stop the blow-by gas from returning to the intake manifold. The unplugged PCV valve experiments were carried out to understand whether PCV blow-by return gas would affect the emissions. After each experiment was finished, the engine was cranked continuously for at least 20 seconds to get rid of the residual fuel as much as possible. Afterwards, the engine was left static for a given time before the next experiment. The engine coolant temperature ranged from 18 to 23 °C throughout the entire experiment process. The cold start experiments were carried out with both gasoline and iso-pentane. When switching fuel, a steady firing of the engine was carried out to assure the complete switch of fuel.

Powertrain Control Parameters

A group of fixed powertrain control parameters for the first 5 firing cycles was defined and applied for each cold start experiment. With firing order 1-3-4-2, cylinder 3 was set to be the first one to fire and cylinder 1 the last. The fuel rail pressure (FRP) was controlled by a PI control module, and the target setpoint was set to 70 bar for the first 5 firing events, and 160 bar afterwards. A dual injection strategy was used in this cold start research. The early injection, taking place during the intake stroke, started at 220 crank angle degrees (CAD) before top dead center (BTDC). The late injection, taking place during the compression stroke, ended at 45 degrees BTDC. The spark ignition timing was set to 10 degrees BTDC for the first firing cycle, -10 degrees BTDC for the 2nd firing cycle, and -20 degrees BTDC for the 3rd to 5th firing cycles. This spark timing setup aimed to allow the engine to reach the targeted engine speed, and switch to the catalyst heating operation mode, a retarded spark-timing mode used by the engine during cold start to heat the exhaust three-way catalyst to light-off temperature. The injection duration split ratio between early and late injection was kept 1:1, and the injection duration was given a decreasing trend to compensate for the increasing FRP during the cold start. The powertrain control parameters were validated before this cold start research to be free from misfiring or weak combustion. If the targeted firing cycle number was smaller than 5, the engine powertrain actions would stop as soon as the targeted firing cycle number was reached, and the un-fulfilled firing events would not be run. The full list of parameters is shown in Table 2.

Table 2 Injection and Spark Parameters for the First 5 Firing Cycles of Cold Start

Firing Cycle	Cylinder #	Firing event order	Injection timing	Intake stroke duration (ms)	Compression stroke duration (ms)	Spark timing (CAD BTDC)	Fuel rail pressure set point (bar)
1	3	1	Intake stroke injection Start-of-Injection timing: 220 CAD BTDC Compression stroke injection End-of-Injection timing: 45 CAD BTDC	2.1	2.1	10	70
	4	2		2.1	2.1	10	
	2	3		1.7	1.7	10	
	1	4		1.7	1.7	10	
2	3	5		1.35	1.35	-10	
	4	6		1.25	1.25	-10	160
	2	7		1.1	1.1	-10	
	1	8		1.0	1.0	-10	
3	3	9		0.95	0.95	-20	
	4	10		0.95	0.95	-20	
	2	11		0.95	0.95	-20	
	1	12		0.95	0.95	-20	
4	3	13		0.9	0.9	-20	

	4	14		0.9	0.9	-20	
	2	15		0.9	0.9	-20	
	1	16		0.9	0.9	-20	
5	3	17		0.9	0.9	-20	
	4	18		0.9	0.9	-20	
	2	19		0.9	0.9	-20	
	1	20		0.9	0.9	-20	

Results and Discussion

The instantaneous engine speed and the transient fuel rail pressure change during a typical cold start as shown in Figure 2. The engine was cranked at an average speed of approximately 300 RPM before the first firing cycle, then during the first firing cycle with advanced spark timing, the engine speed rose quickly to roughly 1100 RPM, which was maintained through the 2nd firing cycle. Starting from the 3rd firing cycle, the engine speed started to drop as the spark timing was retarded to the catalyst heat-up mode of 20 degrees after TDC. The fuel rail pressure was boosted to roughly 80 bar before the first firing event took place and was further pushed upwards in the 2nd and 3rd firing cycles. The fuel rail pressure dropped back to the target fuel rail pressure of 160 bar by the 5th firing cycle where it stabilized. The varying engine speed and the fuel rail pressure played an important role in the cold start emissions.

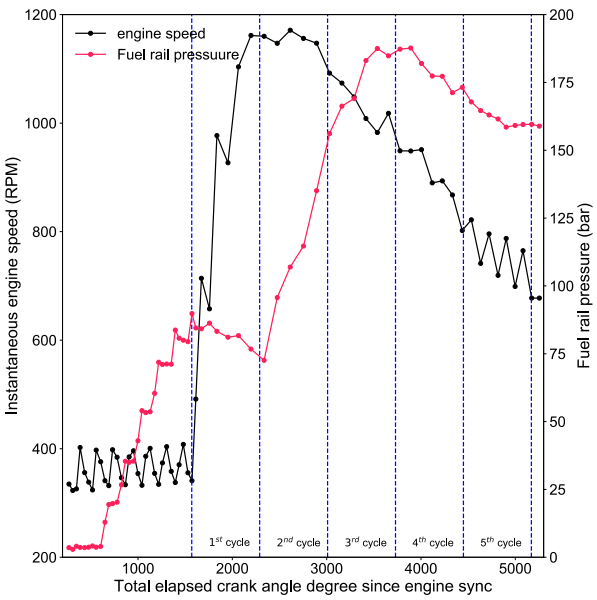

Figure 2 Instantaneous engine speed and fuel rail pressure change during cold start

As a check to ensure that the expected amount of exhaust gas was collected, the volume of gas collected was compared with the calculated amount based on the engine displacement and known intake valve closing crank angle along with the measured number of cranking cycles. The experimentally obtained volumes versus number of cycles is given in Figure 3 along with the calculated volume of gas. During cranking, the intake manifold pressure remained atmospheric. The default IVC timing was 71.1 degrees after bottom dead center (BDC), with intake valve lift 0.43 mm. In theory, the gas volume captured by the collection cylinder each cycle should be equal to the remaining cylinder swept volume at the moment the gas exchange between intake manifold and cylinder was cut-off. The cut-off timing was first assumed to be IVC, for which the calculations were made and compared with the experimental data.

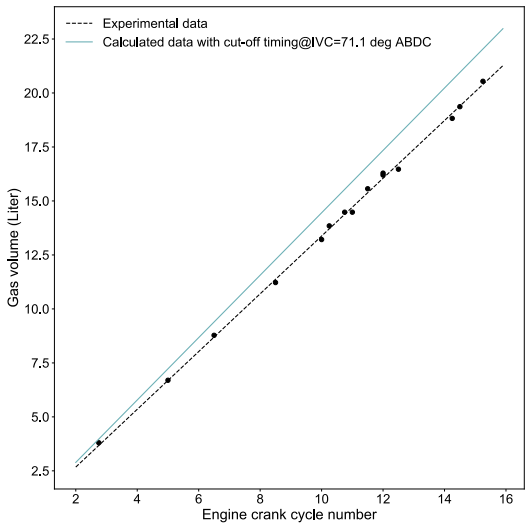

Figure 3 Experiment obtained gas volume versus theoretic calculation results

The experimental captured gas volume increased linearly with the cycle number, indicating consistency in per-cycle engine emission volume. The captured volume was consistently lower, though by less than 10%, than the cylinder remaining sweeping volume values assuming IVC as the cut-off timing. From the results above, the gas

collection equipment could be regarded valid in terms of collecting exhaust gas emitted from the exhaust manifold.

The cumulative emissions of measured HC, CO and CO_2 for different cold start cycles are shown in several following figures. The cumulative emissions from both gasoline and iso-pentane are shown. The bar plots represented the averaged values of 5 (or 6, for the cumulative 5-firing-cycle scenario) experiments. The solid color bar represents the emission mass of a given component captured during the cold start, and the tilted-line-hatched bar plots represent the emission mass captured during the post-cold start cranking process. The error bars indicate the standard deviation of the cold start emissions and post-cold start cranking emissions, respectively.

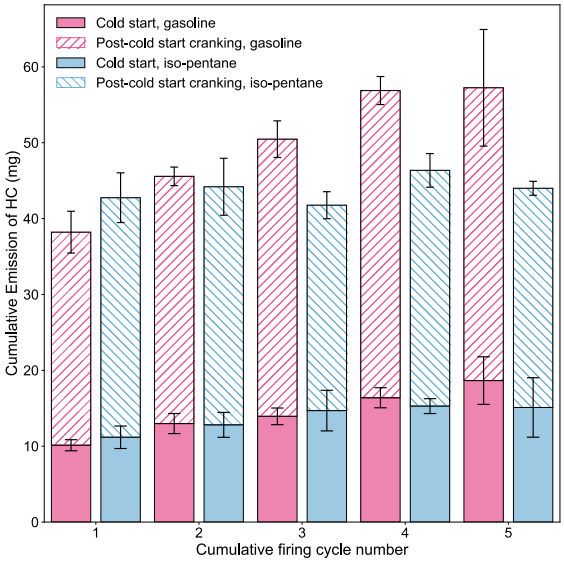

Figure 4 Cumulative HC emissions at 1 to 5 firing cycles

The measured cumulative HC emissions for the first 5 firing cycles are shown in Figure 4. More HCs were collected during the post-cold start cranking step than that emitted from the cold start itself. Among the post-cold start cranking HCs collected were contributions from previous cold start events, either unburned or not fully oxidized fuel. Possible sources include residual fraction either retained in-cylinder or back-flowed into the intake manifold during valve overlap then returned to the cylinder during the subsequent intake stroke, blowby to the crankcase, and even the lubrication oil. For the gasoline, the cumulative HC emissions increase slowly but continuously after the first cycle indicating less HC generation as cycle number increased. For iso-pentane the, cumulative HC emissions leveled out after the first cycle, implying an overwhelming portion of the HCs generated with iso-pentane originated from the first firing cycle.

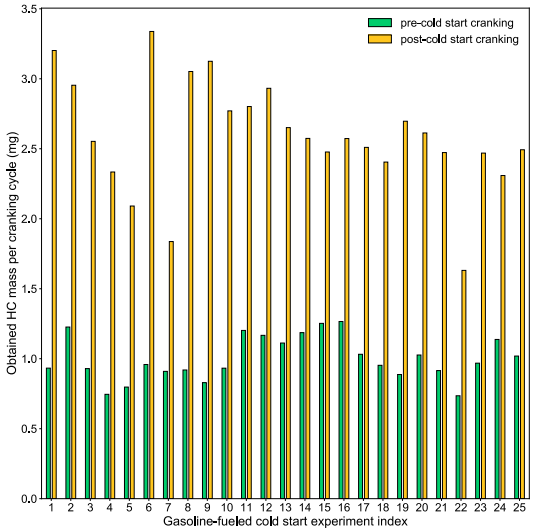

Figure 5 Captured HC mass per-cycle for pre-cold start cranking and post-cold start cranking

While post-cold start cranking could force out the combustion-produced HCs remaining in-cylinder, the post-cold start cranking also brought out other residual HCs deposited, as well. A validation check was necessary to show that the HCs captured during the post-cold start cranking originated from the prior cold start. Captured HC per-cycle mass in the pre-cold start cranking and post-cold start cranking for each gasoline-fueled cold-start experiment is shown in Figure 5. The measured pre-cold start cranking HC level consistent ranged from 0.6 mg/cycle to 1.3 mg/cycle, while the post-cold start cranking step saw a significantly higher per-cycle HC level, varying between 1.6 mg/cycle to about 3.3 mg/cycle. Such differences in the HC emissions level indicated that a major part of the HC captured during the post-cold start cranking was generated during the cold start firing event, and that using the sum of both HC emissions to represent the HC emissions level was reasonable, despite the inevitable inclusion of HC emissions from earlier cold start events and other sources.

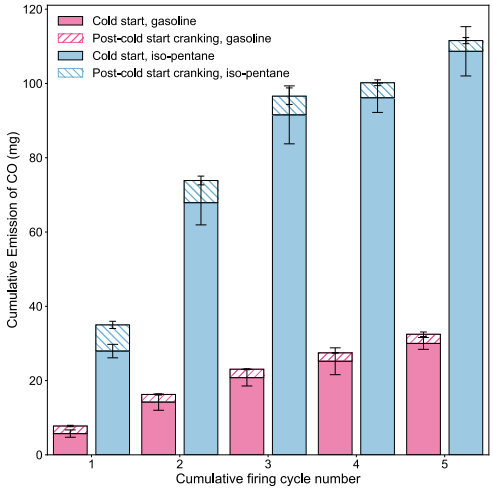

Figure 6 Cumulative CO emissions at 1 to 5 firing cycles

The cumulative CO emissions for firing cycles 1 to 5 are shown in Figure 6. Unlike HCs, which were invariably captured every time the

engine was cranked, the majority of the CO collected via the post-cold-start cranking step was from the cold start combustion reactions. Although there exists the possibility that CO could be generated during the post-cold start cranking process from the intermediate products of incomplete combustion, considering the low in-cylinder temperatures and shortness of the cold start, all CO captured during post-cold-start cranking was believed to be generated solely from the preceding firing combustion cycles. The vast majority of CO was captured during the cold start event itself, with only a small fraction collected during the post-cold start cranking, presumably due to retained residual fraction. In the 1-firing cycle scenario, CO obtained via post-cold start cranking cycles accounted for about 26% and 20% of total collected CO mass for gasoline-fueled and iso-pentane-fueled cold starts respectively. Such values decreased as the cumulative firing cycle number increased and were reduced to 7% and 2% respectively by the 5th firing cycle.

The gasoline-fueled cold-starts generated lower CO levels compared with those of iso-pentane. In the gasoline-fueled cold starts, the cumulative CO emissions increased with a nearly linear trend, yielding a level of 4~8 mg CO generation for each cycle. There were higher CO emissions in the first two cycles, with individual-cycle averages of 7, 8, and 6 mg of total CO captured in the first 3 firing cycles. An average of 4.4 mg of CO was generated during the 4th firing cycle and 5 mg of CO generated during the 5th firing cycle. For the iso-pentane-fueled cold-starts, the cumulative CO emissions increased swiftly for the first three firing cycles, before tapering off beginning with the 4th firing cycle. A large amount of CO was generated during the first 3 firing cycles, with an individual-cycle average of 34, 38, and 22 mg of CO generated. An average of only 4 mg of CO was generated during the 4th firing cycle and 11 mg of CO generated during the 5th firing cycle. The CO emissions were strongly tied to the combustion equivalence ratio (Φ). The higher the Φ, the higher the CO emissions. It was not possible to know the local and temporally dependent equivalence ratio in-cylinder. An alternative was to calculate the global equivalence ratio based on inducted air mass and injected fuel amounts. This is defined as the fuel-air ratio based on the injected fuel mass and the in-cylinder air mass, divided by the stochiometric fuel-air ratio of the fuel:

$$\Phi = \frac{m_f/m_{\text{air}}}{(m_f/m_{\text{air}})_{\text{sto}}} = \frac{\text{AFR}_{\text{sto}}}{\text{AFR}} \qquad (.)$$

The cold start injection equivalence ratio data is shown in Figure 7. The results show that injection equivalence ratio decreased from larger than 1 to smaller than 1 as the cycle index increased, indicating a rich-to-lean combustion change. For gasoline-fueled cold starts, injection Φ decreased from 1.4 for the 1st firing cycle to slightly higher than 1 starting with the 2nd firing cycle. The decrease in Φ and the leaner injection mixture correlated with decreasing CO emissions as the cycle index increased. While injection Φ decreased to approximately 1 starting at the 2nd firing cycle, the CO emissions did not decrease until the 3rd firing cycle. A possible explanation was the carryover of fuel from the previous firing cycle to the combustion in the next firing cycle. For iso-pentane-fueled cold starts, the injection Φ started to decrease from the 2nd firing cycle, yet the CO emissions remained high until the 4th firing cycle. Iso-pentane is highly volatile, and is regarded to fully evaporate as soon as it was injected. Hence, no significant fuel carryover should take place. A possible explanation for the high CO emissions could be the dual injection strategy. The late compression stroke injection created a rich mixture near the spark plug, which led to a locally rich combustion region and high CO emissions. It was not until the 4th firing cycle that local Φ near the spark plug was lean enough and less CO was generated

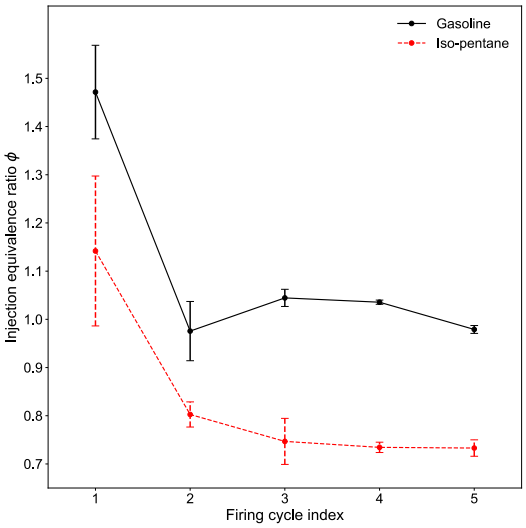

Figure 7 Average injection equivalence ratio for firing cycles 1 to 5

The cumulative CO_2 emissions for firing cycles 1 to 5 for both gasoline and iso-pentane cold starts are shown in Figure 8. As CO_2 could only be generated by cold-start combustion, not in post-cold start cranking, CO_2 captured both during firing and during post-cold-start cranking was generated during the cold-start firing cycles. Like CO, part of cold-start CO_2 generated was not collected during the cold start process, and only captured in the post-cold start cranking. In the 1-firing cycle scenario, the cold-start uncaptured CO_2 accounted for 22% of total collected CO_2 for both gasoline- and iso-pentane-fueled cold starts. In scenarios with higher cumulative firing cycle numbers, the values decreased and reduced to 11% and 6% for the 5-firing cycle scenario in gasoline and iso-pentane cold starts, respectively. For both gasoline and iso-pentane cold-starts, the CO_2 emissions increased linearly, indicating that a consistent amount of CO_2 was generated during each firing cycle. However, iso-pentane-fueled cold-starts generated more CO_2 in each firing cycle. This was because iso-pentane had higher volatility and all of the injected iso-pentane was believed to evaporate and combust, while a significant fraction of the gasoline remained liquid and did not participate in the combustion reaction during the cold-starts.

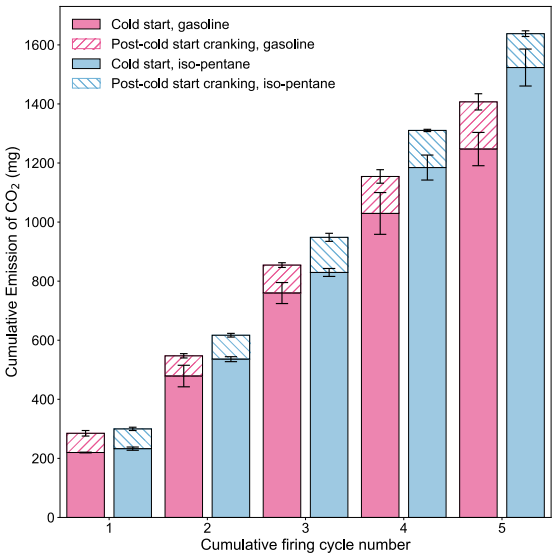

Figure 8 Cumulative CO_2 emissions at firing cycles 1 to 5

There were concerns about whether flow through the PCV valve, which allowed the crankcase blow-by gas to re-enter the intake manifold, would affect the emissions during cold starts. To examine this issue, we have plotted all of the cumulative total cold-start emissions (the emissions captured during the cold start plus the emissions captured during the post-cold start cranking step) data, with their mean and standard deviation in Figure 9. The cold start experiment cases in which the engine PCV valve was disconnected (unplugged) from the intake manifold are marked with blue dots, while the plugged (connected) data points are marked with yellow dots. Different y-axis scales were used as cumulative emissions for the three species were different. The error bars represented one standard deviation of the 5 (or 6, in 5 cumulative firing cycle experiments) experimental data sets. The results show that most of the experimental cases in which the PCV valve was disconnected did not show a statistically significant difference in emissions, with most of the data points lying within one standard deviation difference from the mean values. It was concluded that the PCV valve status did not affect the emissions during cold-starts.

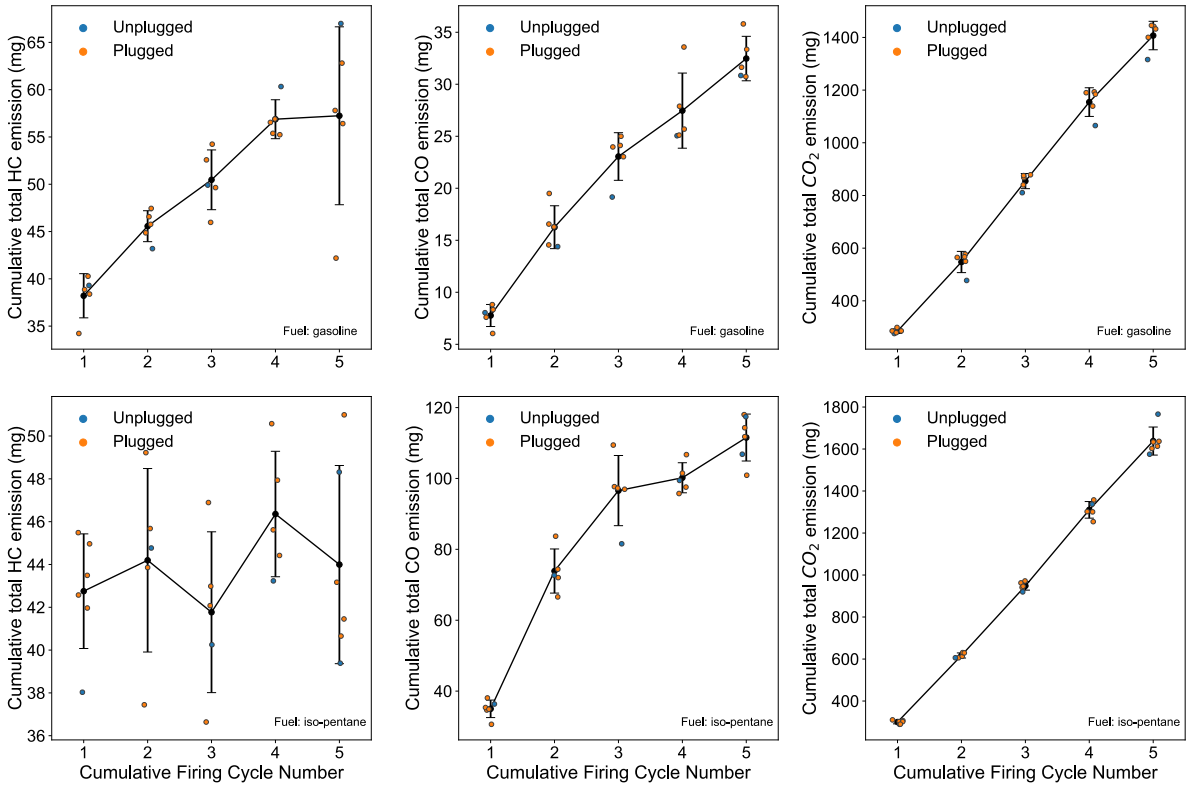

Figure 9 Cumulative emissions scatter data, with PCV valve disconnected (unplugged) data identified

To better understand where the elemental fuel carbon ends up during the cold starts, the cumulative injected carbon was compared with the total captured carbon mass in the form of HCs, CO, and CO_2; this is shown in Figure 10 for both gasoline- and iso-pentane cold-starts. The term carbon conversion rate is defined here to further analyze the experimental data. The carbon conversion rate is defined as the ratio of the carbon elemental mass captured in the exhaust gas over the carbon elemental mass injected into the cylinder. Two carbon conversion rate indicators were calculated. The first one, whose values are shown without parentheses in Figure 10, was based on the elemental carbon mass solely captured during the cold start. This indicator was named the lower conversion rate of carbon (LCR). The other indicator, whose values are shown between parentheses, is based on the total captured carbon in both cold-start and post-cold-start cranking. This indicator is named the higher conversion rate of carbon (HCR).

$$\text{LCR} = \frac{m_{\text{C,firing}}}{m_{\text{C,inj}}} \times 100\% \qquad (.)$$

$$\text{HCR} = \frac{m_{\text{C,firing}} + m_{\text{C,post-cold start cranking}}}{m_{\text{C,inj}}} \times 100\% \qquad (.)$$

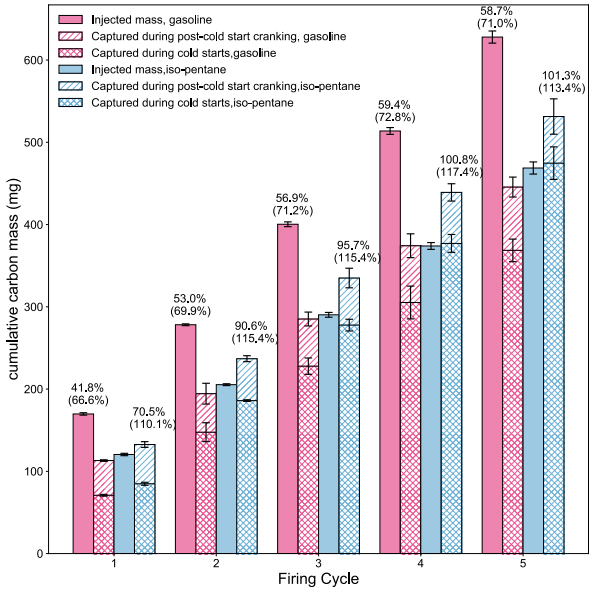

Figure 10 Cumulative carbon elemental mass injection and capture comparison

The difference between HCR and LCR was mainly due to the uncaptured CO and CO_2 during the cold-start. Part of the difference between the HCR and the LCR, however, was due to previously deposited fuel from earlier cold-start events and captured as the carbon evolved during the post-cold-start cranking. This contribution, however, was not significant, and became less significant as the firing cycle increased. Uncaptured HCs (either not fully combusted or not combusted at all), CO, and CO_2 from the preceding cold start dominated the HCR-LCR difference. The HCR was used for further carbon mass capture analysis.

The cumulative LCR and HCR increased as the firing cycle number increased for both gasoline- and iso-pentane-fueled cold starts. For gasoline-fueled cold starts, the LCR increased from roughly 40% for a 1-firing-cycle scenario to 58% in the 4-firing-cycle scenario and changed little in the 5-firing-cycle scenario, while the HCR increased from about 66% to about 71% after 5 firing cycles. Note that these are cumulative amounts over the actual number of fired cycles. Such increases with the number of fired cycles might result from the change in-cylinder surface temperatures which led to more gasoline evaporation. Another possible reason for higher HCR and LCR values would be the carryover of the unburnt gasoline from the previous firing cycles to the current firing cycle. Part of the gasoline carried over may have been injected in the previous cycle yet not evaporated and burned until the current cycle, while another contribution may have been gasoline from even earlier injections or previous cold-start events that gradually volatizes.

For iso-pentane-fueled cold starts, the cumulative HCR was already above 110% for the 1-firing-cycle scenario, and remained above 110% for scenarios with 2 or more cumulative firing cycles. The higher than 100% HCR indicates that residual HC sources, possibly gasoline in the crankcase or in the cylinder, either joined the combustion, or was collected during the experimental process. The low LCR in the 1-firing-cycle scenario was because there were few inertia cycles following the single firing event of the cold start and not all of the exhaust residual was pushed out to the collection cylinder. The gas was afterwards pushed out during the post-cold start cranking process. It should be noted that LCRs in 4- or 5-firing-cycle scenarios were approximately 100%. This does not mean that all of the iso-pentane injected was burned and collected during the cold start, however. During the cold start, all of the iso-pentane plus part of the historic residual HCs joined the combustion, of which a large portion of the products got collected and measured. The rest of the cold start products, plus some historic HCs, got collected during the post-cold start cranking step, and that captured carbon added to the previously captured carbon to form HCR.

The high HCR for iso-pentane-fueled cold starts validated the current analysis methodology and shows that the low fractions of collected carbon for gasoline operation was not due to a major measurement error. The comparison of gasoline-fueled and iso-pentane-fueled results also suggest that the low HCR values for gasoline operation were presumably due to gasoline that remained in-cylinder as liquid gasoline, and therefore, did not join the combustion, possibly forming a wet film, or passed by the piston rings to the crankcase.

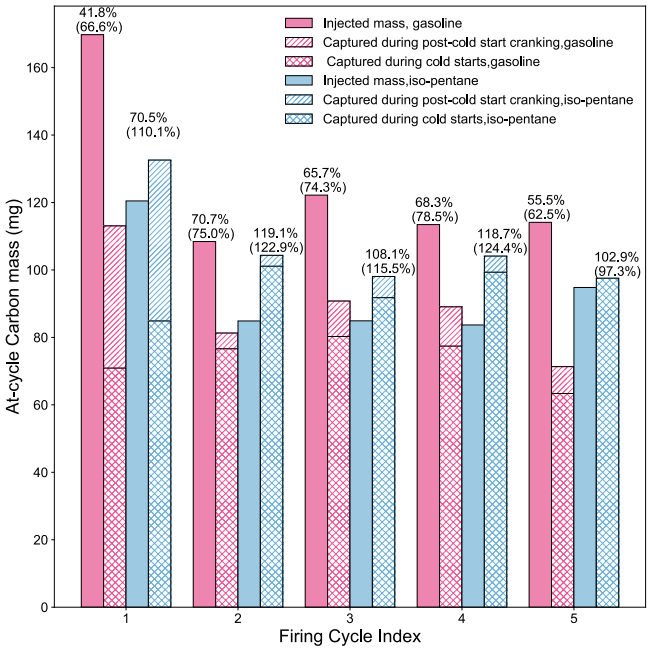

Figure 11 At-cycle carbon elemental mass injection and capture comparison

The cycle-by-cycle carbon elemental mass injected and captured for each firing cycle was calculated and plotted in Figure 11. For the gasoline-fueled cold start data, an obvious fuel carryover phenomenon was observed between the 1st and 2nd firing cycles, with a huge increase in HCR/LCR for the 2nd firing cycle. The individual cycle HCR/LCR achieved relatively high values in the 2nd ,3rd, and 4th firing cycles before dropping lower by the 5th firing cycle, implying possible fuel carry-over phenomena over these firing cycles. For iso-pentane operation, the individual cycle HCR/LCR was consistently higher than 100% for the 2nd, 3rd, and 4th firing cycles, which may be explained by historic HC deposits joining the combustion. The sudden evolution of historic HC deposits being combusted could be

explained by the fact that the engine speed rose rapidly and wall surface temperatures began to increase after the 1st firing cycle. The in-cylinder environment provided favorable conditions for the historic fuel deposits to join the oxidation combustion. The decrease in individual cycle HCR and LCR levels by the 5th firing cycle might be caused by the decreasing engine speed and the weakened in-cylinder combustion conditions as the spark ignition timing was retarded. The HCR was smaller than the LCR by the 5th firing cycle. Such an abnormality was not impossible and indicates a smaller amount of carbon captured during the post-cold-start cranking steps for the 5 cumulative firing cycle scenario compared with the 4th cycle scenario. In absolute value, the difference was 8 mg, small enough to be within the measurement uncertainty.

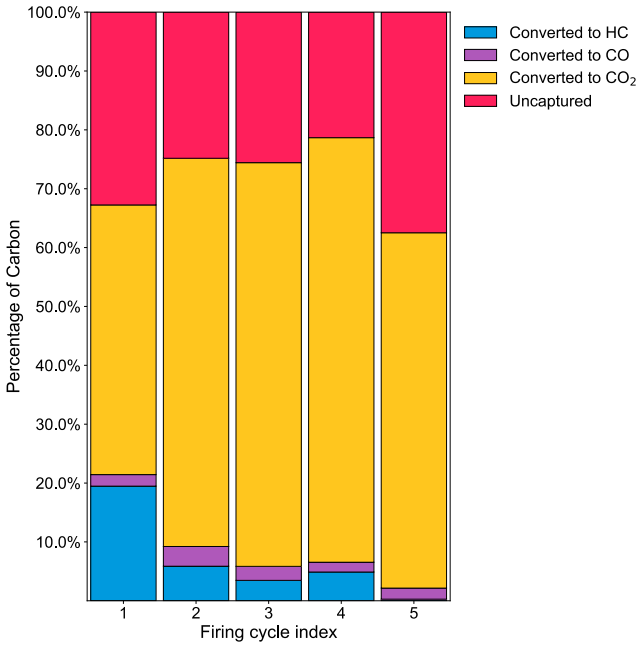

Figure 12 Percent carbon distribution for each individual firing cycle in the gasoline-fueled cold starts

The carbon elemental distribution among species in each firing cycle for gasoline-fueled cold-starts is shown in Figure 12. The emissions of HCs, CO, and CO_2 were calculated based on the gas mass captured for the cold start event and the post-cold start cranking step. The calculation did not include the contribution of historic HC deposits and gasoline carried over from the previous cycle, whether combusted or not. The effect of these additional HC sources was not possible to quantify for now. Most of the carbon mass in the gasoline was converted to CO_2 as expected. The conversion to HCs was greatest for the 1st firing cycle, with 20% of the carbon emitted as HCs. The amount of carbon converted to HCs dropped to less than 5% starting from the 2nd firing cycle, and almost 0% by the 5th firing cycle. The uncaptured carbon accounted for roughly 33% for the 1st firing cycle, and was at least 20% for the following cycles. Such results indicated a low rate of liquid-to-vapor conversion for gasoline for the first few firing cycles, with the HCR between 66% and 78%. Because carried-over fuel and historic HCs were believed to join the combustion, the measured HCR values are believed to overestimate the ratio of carbon converted from liquid to vapor during the cold start process.

Summary and Conclusions

A cold-start experiment featuring gasoline and iso-pentane as fuel was carried out for the first 5 firing cycles with predetermined powertrain control parameters. Exhaust gas from the cold-start, the pre-cold-start cranking step, and the post-cold-start cranking step was measured using validated measurement equipment. The following conclusions were drawn based on the experimental results.

1. The engine speed rose quickly during the 1st firing cycle to roughly 1100 rpm with 10 degrees BTDC spark timing. Starting from the 2nd firing cycle, the engine speed was reduced gradually as the spark timing was retarded. The fuel rail pressure rose to a middle value of roughly 70 bar by the 1st firing cycle and then rose further to roughly 160 bar for the following 4 firing cycles.
2. More HCs were captured during the post-cold start cranking process than the cold start process itself, for both gasoline and iso-pentane fueled cold starts. Besides the generation of HCs during the cold-start, collected HCs could come from previously deposited HC sources from the cylinder/crankcase, or they could have come from fuel carried over from the previous cycles. The post-cold-start-cranking-collected HCs had a significantly higher per-cycle captured mass compared with pre-cold-start cranking, proving that the majority of HCs obtained during the post-cold start cranking step were due to carry-over from the cold-start event.
3. Both CO and CO_2 captured during the post-cold-start cranking could only be generated during the cold start firing, and hence should be directly added to the amounts collected during the cold start. Post-cold start-cranking-collected CO and CO_2 accounted for a small portion of the overall CO and CO_2 emissions. For the 1-firing cycle cold starts, post-cold start cranking-collected CO and CO_2 accounted for 26% and 22% of the total collected CO and CO_2 carbon mass, respectively. For other firing cycle scenarios, it accounted for less than 12% of the total collected CO (or CO_2) mass.
4. For gasoline-fueled cold starts, the cumulative HC emissions increased at a slowing rate, indicating less HCs being generated as the cycle number increased. The cumulative CO and CO_2 emissions increased at a nearly linear rate. For iso-pentane-fueled cold-starts, the cumulative HC emissions remained unchanged as the firing cycle number increased, implying that most of the HCs were generated during the 1st firing cycle. The cumulative CO emissions for iso-pentane-fueled cold- starts showed a slowing rate of increase, while the cumulative CO_2 emissions showed a linear increase with cycle number.
5. Disconnecting the PCV valve hose from the intake manifold had no measurable impact on emissions for the first 5 firing cycles.
6. Gasoline-fueled cold-starts had a significant portion of the gasoline uncaptured. Such missing carbon indicated a slow rate of gasoline vaporization during the cold start. Iso-pentane, with its low boiling point, was highly volatile and appeared to fully evaporate and take part in combustion during the cold-starts. The iso-pentane-fueled cold-starts obtained carbon conversion rates higher than 100%, implying the participation of additional HC sources into the combustion reactions.
7. The individual-cycle carbon conversion data showed that for gasoline fueling, the fuel not evaporated, and therefore not burned in the previous cycles could be carried over to the current cycle and burned there.
8. The gasoline-fueled cold-starts had individual-cycle carbon conversion rates between 66% and 78%which meant that between 22% and 34% of the injected fuel remained unvolatilized for the first 5 firing cycles; thus, a significant fraction of the gasoline failed to evaporate and burn. Given that it was not possible for now to

quantify the full effects of historic HC deposits and previous gasoline carry-over phenomena, the portion of unconverted gasoline could have been even higher.

References

1. Zhao, F., Lai, M.C., and Harrington, D.L., "Automotive spark-ignited direct-injection gasoline engines," *Progress in Energy and Combustion Science* 25(5):437–562, 1999, doi:10.1016/S0360-1285(99)00004-0.

2. Queiroz, C. and Tomanik, E., "Gasoline Direct Injection Engines - A Bibliographical Review," 973113, 1997, doi:10.4271/973113.

3. Peckham, M.S., Finch, A., and Campbell, B., "Analysis of Transient HC, CO, NOx and CO2 Emissions from a GDI Engine using Fast Response Gas Analyzers," *SAE Int. J. Engines* 4(1):1513–1522, 2011, doi:https://doi.org/10.4271/2011-01-1227.

4. The 2019 EPA Automotive Trends Report: Greenhouse Gas Emissions, Fuel Economy, and Technology since 1975, United States Environmental Protection Agency, 2020.

5. Tong, K., Quay, B.D., Zello, J.V., and Santavicca, D.A., "Fuel Volatility Effects on Mixture Preparation and Performance in a GDI Engine During Cold Start," SAE Paper 2001-01–3650, 2001, doi:10.4271/2001-01-3650.

6. Burke, D., Foti, D., Haller, J., and Fedor, W.J., "Fuel Rail Pressure Rise during Cold Start of a Gasoline Direct Injection Engine," 2012-01–0393, 2012, doi:10.4271/2012-01-0393.

7. Wiemer, S., Kubach, H., and Spicher, U., "Investigations on the Start-Up Process of a DISI Engine," SAE Technical Paper 2007-01–4012, SAE International, Warrendale, PA, 2007, doi:10.4271/2007-01-4012.

8. Xu, Z., Yi, J., Wooldridge, S., Reiche, D., Curtis, E.W., and Papaioannou, G., "Modeling the Cold Start of the Ford 3.5L V6 EcoBoost Engine," *SAE Int. J. Engines* 2(1):1367–1387, 2009, doi:10.4271/2009-01-1493.

9. Fan, Q. and Li, L., "Transient Characteristics of Cold Start Emissions from a Two-Stage Direct Injection Gasoline Engines Employing the Total Stoichiometric Ratio and Local Rich Mixture Start-up Strategy," 2012-01–1068, 2012, doi:10.4271/2012-01-1068.

10. Fan, Q., Bian, J., Lu, H., Li, L., and Deng, J., "Effect of the fuel injection strategy on first-cycle firing and combustion characteristics during cold start in a TSDI gasoline engine," *Int.J Automot. Technol.* 13(4):523–531, 2012, doi:10.1007/s12239-012-0050-3.

11. Imatake, N., Saito, K., Morishima, S., Kudo, S., and Ohhata, A., "Quantitative Analysis of Fuel Behavior in Port-Injection Gasoline Engines," 971639, 1997, doi:10.4271/971639.

12. Rodriguez, J.F. and Cheng, W.K., "Effect of Operation Strategy on First Cycle CO, HC, and PM/PN Emissions in a GDI Engine," *SAE International Journal of Engines* 8(3):1098–1106, 2015, doi:10.4271/2015-01-0887.

13. Rodriguez, J.F. and Cheng, W.K., "Reduction of Cold-Start Emissions through Valve Timing in a GDI Engine," *SAE Int. J. Engines* 9(2):1220–1229, 2016, doi:10.4271/2016-01-0827.

14. Titus, F., Berlet, P., Sobek, F., and Wessling, J., "Emission Reduction during Cold Start by Combustion Controlled Increase of In-Cylinder Temperatures," SAE Paper 2018-01–1740, 2018, doi:10.4271/2018-01-1740.

15. Kim, S.-J., Hyun, S., and Park, J., "Optimization of Cold Start Operating Conditions in a Stoichiometric GDI Engine with Wall-guided Piston using CFD Analysis," SAE Paper 2013-01–2650, 2013, doi:10.4271/2013-01-2650.

16. Malaguti, S., Cantore, G., Fontanesi, S., Lupi, R., and Rosetti, A., "CFD Investigation of Wall Wetting in a GDI Engine under Low Temperature Cranking Operations," SAE Paper 2009-01–0704, 2009, doi:10.4271/2009-01-0704.

17. Malaguti, S., Fontanesi, S., and Severi, E., "Numerical Analysis of GDI Engine Cold-Start at Low Ambient Temperatures," SAE Paper 2010-01–2123, 2010, doi:10.4271/2010-01-2123.

18. Hu, J., Hall, M., Matthews, R., Moilanen, P., Wooldridge, S., and Yi, J., "A Novel Technique for Measuring Cycle-Resolved Cold Start Emissions Applied to a Gasoline Turbocharged Direct Injection Engine," *SAE Int. J. Adv. & Curr. Prac. in Mobility* 2(5):2469–2478, 2020, doi:10.4271/2020-01-0312.

Contact Information

Prof. Matthew J. Hall
mjhall@mail.utexas.edu

The University of Texas at Austin
Department of Mechanical Engineering
204 E. Dean Keeton St. C2200
Austin, TX 78712

Acknowledgments

This project was made possible through the funding provided by the Ford Motor Co. through the University of Texas at Austin's Site of the NSF Center for Efficient Vehicles and Sustainable Transportation Systems (EV-STS).

Definitions/Abbreviations

BDC	Bottom dead center
BTDC	Before top dead center
CAD	Crank angle degrees
ECU	Engine control unit
GDI	Gasoline direct injection
GTDI	Gasoline turbocharged direct injection

HC	Hydrocarbons	**TDC**	Top dead center
HCR	Higher conversion rate of carbon		
IVC	Intake valve closing		
PCV	positive-crankcase ventilation		
PFI	Port-fuel injection		
LCR	Lower conversion rate of carbon		